Geol. Mag. **152** (3), 2015, pp. 504–520. © Cambridge University Press 2014
doi:10.1017/S0016756814000491

Allophanic and ferric root-associated stalactites: biomineralization induced by microbial activity (Galeria da Queimada lava tube, Terceira, Azores)

R. DAZA* & M. A. BUSTILLO

Museo Nacional de Ciencias Naturales-CSIC, Calle José Gutiérrez Abascal 2, 28006 Madrid, Spain
(abustillo@mncn.csic.es)

(*Received* 20 February 2014; *accepted* 4 August 2014; *first published online* 29 September 2014)

Abstract – Root-associated stalactites (rootsicles) in Galeria da Queimada lava tube have a mineralogical composition and developmental association with microbes that render them unique. Samples were examined by X-ray diffraction, micro-Raman spectrometry and scanning electron microscopy/X-ray energy-dispersive spectroscopy. Three types of rootsicle were defined: incipient; hard (white and red); and black spongy. The incipient rootsicles still contained rotten organic material and showed the beginning of mineralization by allophane. The white hard and black spongy types were also composed of allophane, while the red hard type was composed of hydrous ferric oxi-hydroxide minerals (HFO). The allophane and HFO in the andisol covering the cave roof precipitated out of the dripwater running along the roots to form the studied rootsicles. All three types of rootsicle showed black layers, coatings, spots or patches composed of manganese oxide minerals and, occasionally, hisingerite (iron (III) phyllosilicate). An alternation of organic precipitation caused by filamentous bacteria and inorganic precipitation (the latter facilitated by pH changes in the dripwater and the cave's temperature) built up both the porous and compact rings observed in the white and red hard rootsicles. The largely straight filaments seen in the porous rings of the white hard rootsicles may be indicative of the previous presence of *Leptothrix* spp., while the helical morphologies seen in the red hard rootsicles may be indicative of that of *Gallionella* spp. The manganese oxide minerals detected probably formed via microbial activity. This study reflects the important role of filamentous bacteria in rootsicle formation, independent of their mineralogy.

Keywords: rootsicles, aluminium silicate, Fe oxi-hydroxides, manganese, filamentous bacteria, speleothem.

1. Introduction

The idea of a role for living organisms in the formation of certain speleothems is not new, but it was not until the second half of the last century that evidence emerged indicating that microorganisms might somehow control their formation (see data in Forti 2001). Recently however, speleothems have been confirmed as having resident populations of microorganisms (Boston *et al.* 2001; Barton & Northup, 2007; Northup *et al.* 2011) and it is now known that their metabolism and biomineralization activities make important contributions to speleothem formation (Forti 2001, 2005; Northup *et al.* 2011). Experimental work has shown that the exopolysaccharides and surface characteristics of microorganisms enhance precipitation rates (Kasama & Murakami, 2001).

Root-associated stalactites (rootsicles) are rare and little-studied speleothems formed from plant roots that penetrate caves with ceilings not far underground. As they grow downwards in their search for water, these roots become fossilized by (generally) calcium carbonate. Different authors have recorded rootsicles in limestone caves (James *et al.* 1982; Jasinska *et al.* 1996; Hill & Forti, 1997; Hill 1999; Taboroši, Hirakawa & Stafford, 2004; Castaño, Redondo Vega & Fernández Martínez, 2010; Tamas & Ugureanu, 2010), lava tubes and, more rarely, in gypsum caves (Hill & Forti, 1997). They have never been studied in detail, but seem to start as lithified roots (Taboroši, Hirakawa & Stafford, 2004). They usually appear as stalactites (alone or in groups) hanging from cave ceilings, but occasionally may be seen running down flowstone surfaces or growing downwards from the uppermost edge of small cave pools (Hill & Forti, 1997). They generally have a beige, brown, reddish or orange colour, and may be 0.5–1.5 m long and 3–4 cm thick (although locally they may be thicker). They may also form columns (James *et al.* 1982). The roots may be entirely obscured leaving only mineral casts (Hill & Forti, 1997).

The above studies report information on rootsicle morphology, size, locations in caves and sometimes even on the formation process, but the literature contains little on biomineralization as part of rootsicle formation.

Earlier studies of the Galeria da Queimada lava tube (Daza & Bustillo, 2013) revealed the presence of different types of speleothem such as stalactites, stalagmites,

*Author for correspondence: raquel.daza@mncn.csic.es

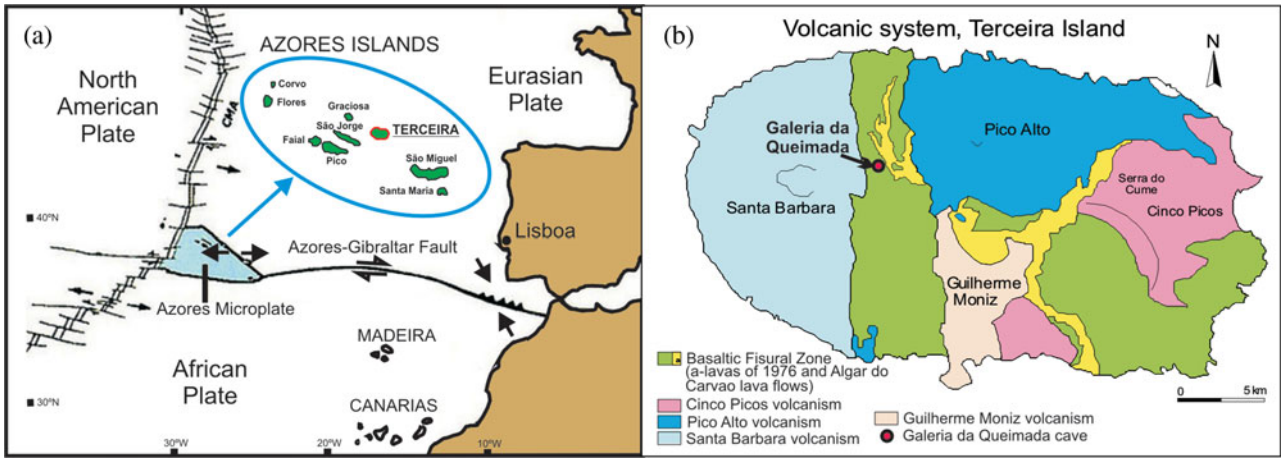

Figure 1. (Colour online) (a) Location of Azores Islands in the tectonic context. (b) Location of the Galeria da Queimada cave on Terceira Island (Azores). Modified from Nunes (2004).

columns, gours and flowstones. However, the rootsicles in this cave were not then recognized as such. The aim of the present work is to characterize the rootsicles of the Galeria da Queimada lava tube in terms of their structure, composition and genesis, taking account of the role of biomineralization in their formation. The observed formation of allophane by microbes in these rootsicles is quite unknown. The present data reveal undocumented types of root-associated speleothems.

2. Geological setting and general remarks

The archipelago of the Azores is located in the North Atlantic Ocean, about 1600 km west of Lisbon, Portugal. It comprises nine volcanic islands organized into three main groups: Flores and Corvo to the west; Graciosa, Terceira, São Jorge, Pico and Faial in the centre; and São Miguel, Santa Maria and the Formigas Reef to the east. The archipelago is located at a triple junction between the Eurasian, African and North American tectonic plates (Fig. 1a). The island of Terceira is in the central group (38° 45′ 42″ N, 27° 5′ 26″ W) and is the largest island of the archipelago (396.75 km^2).

Four polygenetic volcanic systems (Pico Alto, Santa Bárbara, Guilherme Moniz and Cinco Picos) and a basaltic fissural zone that was most active in the NW over the last 50,000 years, can be differentiated on geological maps (Nunes, 2000, 2004) (Fig. 1b). These volcanic systems developed along a prominent NW–SE-oriented fissure zone that transects the island and is part of the Terceira Rift (Self & Gunn, 1976). The exposed rocks on Terceira are all of Late Pleistocene and Holocene age (Calvert *et al*. 2006). Terceira is constructed from stratovolcanoes and abundant, widely distributed basaltic vents. The stratovolcanoes were built up by basaltic-to-trachytic lava flows and pyroclastic deposits, and all have nested summit calderas (França *et al*. 2003; Calvert *et al*. 2006). The lava flows contain cave systems that range from single tubes to branched tubes through to those with dendritic patterns (Nunes *et al*. 2008).

Over the course of a year, the temperature of the island typically varies from 12 °C to 26 °C; it rarely drops below 10 °C or rises much above 28 °C. The relative humidity typically ranges from 63 % to 94 %. The estimated mean annual rainfall of 1085 mm is strongly seasonal, with heavy rains from December until April. The humidity and temperature cause the rapid alteration of pyroclastic, vitric and porous materials, giving rise to abundant formations of amorphous and cryptocrystalline products – a mineralogy typical of andisols. Andisols normally occur under well-defined climatic conditions and form a characteristic ‘stratum’, the altitude limits of which are dependent on climate. Transitional forms such as ferruginous andisols can be found at altitudes above those where andisols typically form, while at lower altitudes ‘brown soils’ may appear (Pinheiro, 2012).

3. The Galeria da Queimada lava tube

The Galeria da Queimada lava cave is located south of Biscoitos in the basaltic fissural zone in the centre of Terceira (Fig. 1b); it is housed within a basaltic lava flow that was emitted from the Picos Gordos scoria cones about 4480 ± 40 years BP (Calvert *et al*. 2006). This tube is 640 m in length, 0.3–2.5 m in height and 0.26–10.9 m wide (Fig. 2). It lies at an altitude of 473 m above sea level (Borges, Pereira & Silber, 1992) in what is now grassland. Near the entrance, the tube splits into two galleries (Fig. 2). The speleothems of the tube are still growing; given their location very close to the ground surface, their growth is influenced by the humid climate.

4. Materials and methods

The distribution of the rootsicles was examined over a 370 m stretch of the lava tube (starting at the tube entrance). Different rootsicles (white, red-orange and black) were sampled throughout the cave (Fig. 2). All sampling was performed in the dry season (summer),

https://doi.org/10.1017/S0016756814000491 Published online by Cambridge University Press

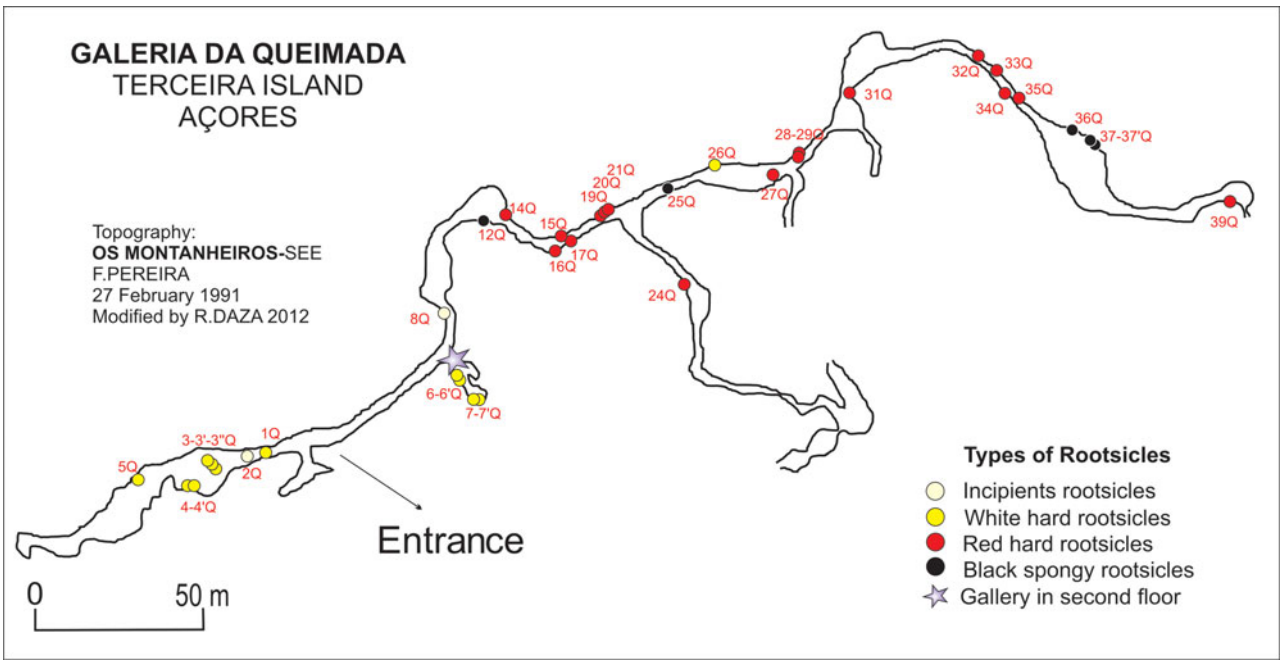

Figure 2. (Colour online) Topography of the Galeria da Queimada lava tube and rootsicle sampling points. Modified from Borges, Silva & Pereira (1992).

since some parts of the cave become partially flooded during the rainy season.

The samples were mineralogically characterized by X-ray diffraction (providing total powder diagrams) using a Philips PW1710 diffractometer with monochromatic CuK α radiation. Micro-Raman spectrometry was performed using a Thermo-Fisher microscope. The mineralogy and textures of the samples were not determined by standard optical microscopy since the samples contained amorphous minerals with a powdery or gelatinous texture. Rather, the identification of these components was made using scanning electron microscopy (SEM) with small fractured samples mounted on stubs coated with a layer of gold. All observations were made using a FEI Inspect microscope, operating at 30 kV at a distance of 10 mm in high vacuum mode, and using secondary electron and backscatter detectors. The instrument used was equipped with an Oxford Analytical-Inca X-ray energy-dispersive system (EDX).

5. Results

5.a. Rootsicle types

The rootsicles observed were aligned with the ceiling cooling-crack system (these cracks are both transversal and longitudinal; Fig. 3a), and were formed from the fine and very fine roots of plants and shrubs growing in the soil overlying the lava tube roof (Fig. 3b). Fresh roots were very scarce; most were rotten and mineralized. The smallest roots probably corresponded to grass roots and the largest to those of brambles and ferns. Some rootsicles involved single roots but more commonly groups of roots (Fig. 3c), producing an intertwined appearance (Fig. 3d). Smaller mineralized threads were visible between the roots and on their surfaces. All showed slight deflections from the vertical axis. They ranged from 5 cm to 60 cm in length; their diameters could not be measured since the rootsicles often took the form of small draperies or complex stalactites (Fig. 3e).

Three types of rootsicle were observed inside the lava tube: (1) incipient rootsicles; (2) hard rootsicles (white and red); and (3) black spongy rootsicles.

5.a.1. Incipient rootsicles

The incipient rootsicles were ochre in colour, translucent, highly porous and showed no external concentric rings. The roots involved mostly appeared rotten and were wrapped with mucus (Fig. 3d). They were very damp and had white spots on their surfaces (bacterial colonies). Their transverse sections were very complex, with anastomosed intercalations of partially mineralized rootlets mixed with a lumpy, wet mass.

5.a.2. Hard rootsicles

The hard rootsicles showed concentric mineral rings arranged axially around one or more roots. These mineral rings were round or ellipsoid in cross-section, and varied in size (although all were <1 mm across). Their outsides were usually less damp than their insides since dripwater passes through the rootsicle body. Two varieties were observed: white (Fig. 3c, d) and red (Fig. 3f).

The white hard rootsicles were opaque or hyaline (Fig. 3c, d) with orange, grey and black patches. Three zones were observed in transverse section (Fig. 4a, b): (1) an interior zone (1–5 mm thick) of ochre-brownish

https://doi.org/10.1017/S0016756814000491 Published online by Cambridge University Press

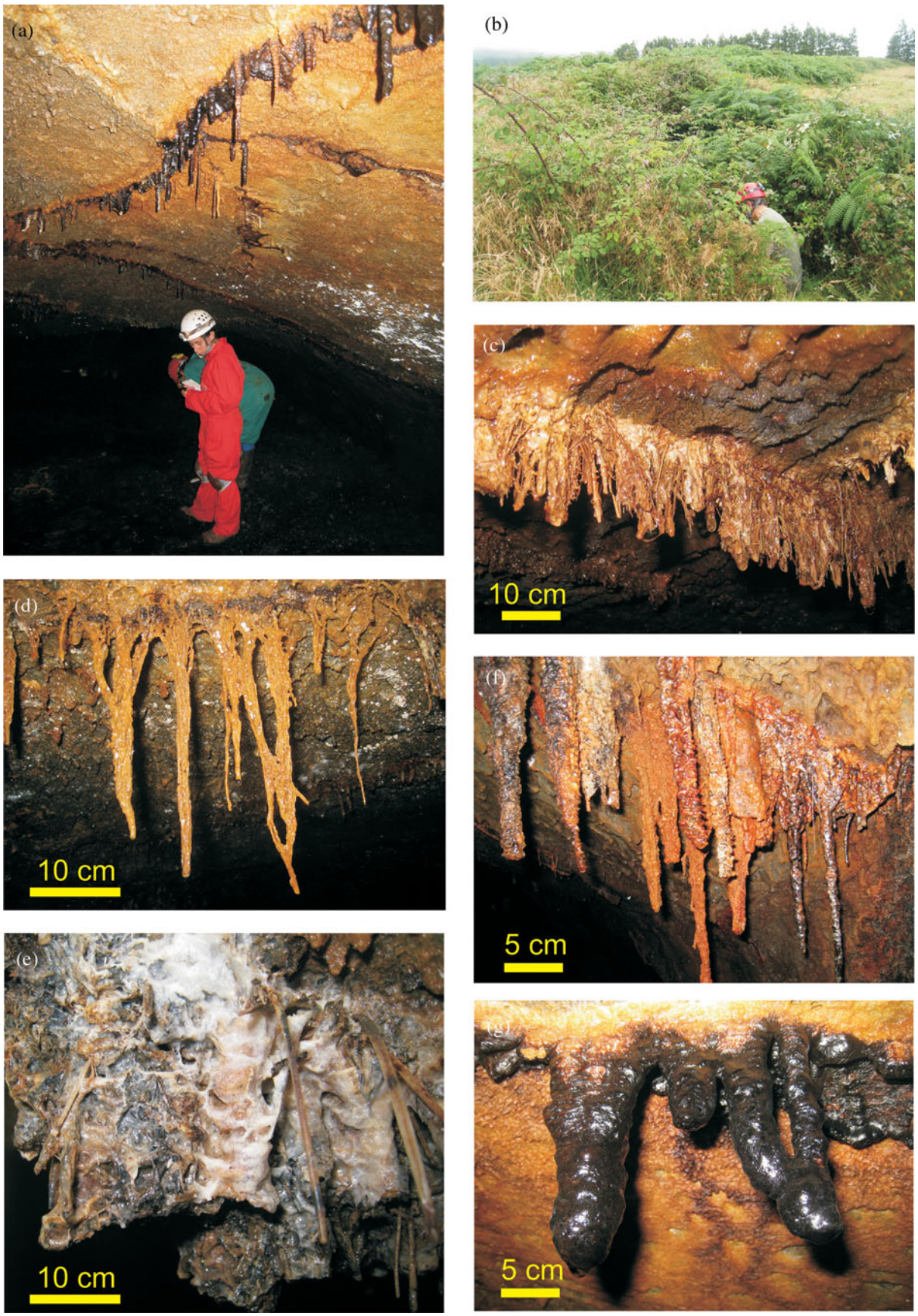

Figure 3. (Colour online) Field photographs of the lava tube and its rootsicles. (a) Rootsicle growth was aligned with the ceiling's cooling cracks (which lie transversally and longitudinally to the axis of the lava tube). (b) Plants (grasses, small plants, ferns and brambles) growing in soil overlying the lava tube roof and at the tube entrance. (c) Anastomosed white hard rootsicles growing from a crack, showing very fine mineralized roots. (d) Intertwined appearance of some incipient rootsicles. (e) Several white hard rootsicles forming small draperies. (f) Red hard rootsicles with black and white patches and 'veins' on their surface. (g) Black spongy rootsicles.

https://doi.org/10.1017/S0016756814000491 Published online by Cambridge University Press

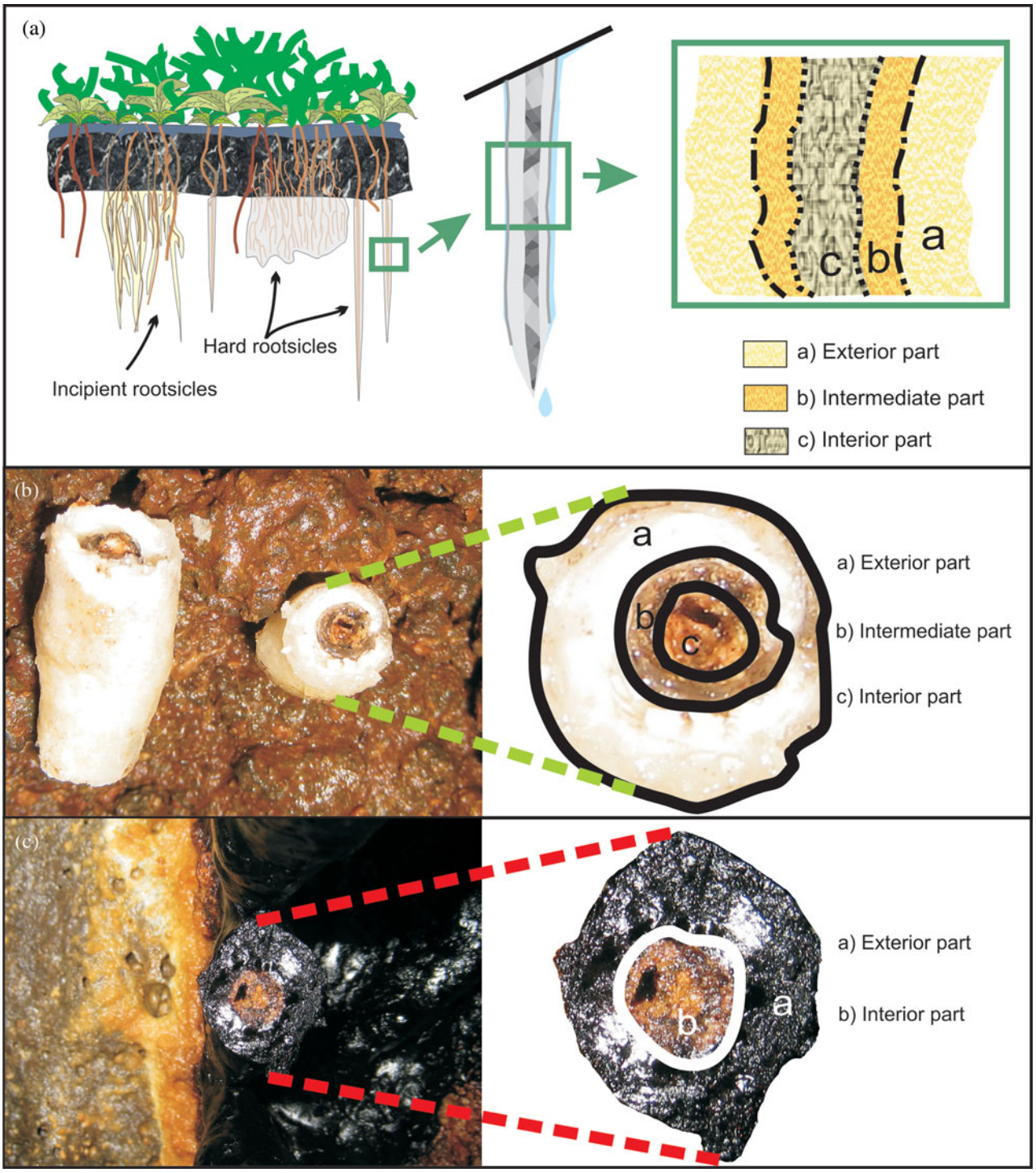

Figure 4. (Colour online) (a) Sketch showing general features of the root-associated stalactites. (b) Transverse section of a white hard rootsicle showing its three zones. (c) Transverse section of a black spongy rootsicle and its two zones.

material with a lumpy texture, including relics of partially or totally mineralized root; (2) an intermediate zone (<1 mm thick), grey in colour and with a ringed structures (black rings marked the boundary between the intermediate and exterior zone); and (3) an exterior zone (0.5–1 cm) consisting of pearly white rings (all of submillimetre thickness).

The red hard rootsicles were formed by intercalations of red, orange and black rings; it was very difficult to discern any of the zones seen in the white rootsicles. Black and white patches or 'veins' were seen at their surface (Fig. 3f). In some cases, the hard rootsicles appeared to be a mixture of the white and red varieties.

5.a.3. *Black spongy rootsicles*

Although mainly black in colour (Fig. 3g), these spongy rootsicles occasionally had a yellow interior (Fig. 4c). Those that were only black had no ringed structure, millimetre-sized holes and a porous texture.

https://doi.org/10.1017/S0016756814000491 Published online by Cambridge University Press

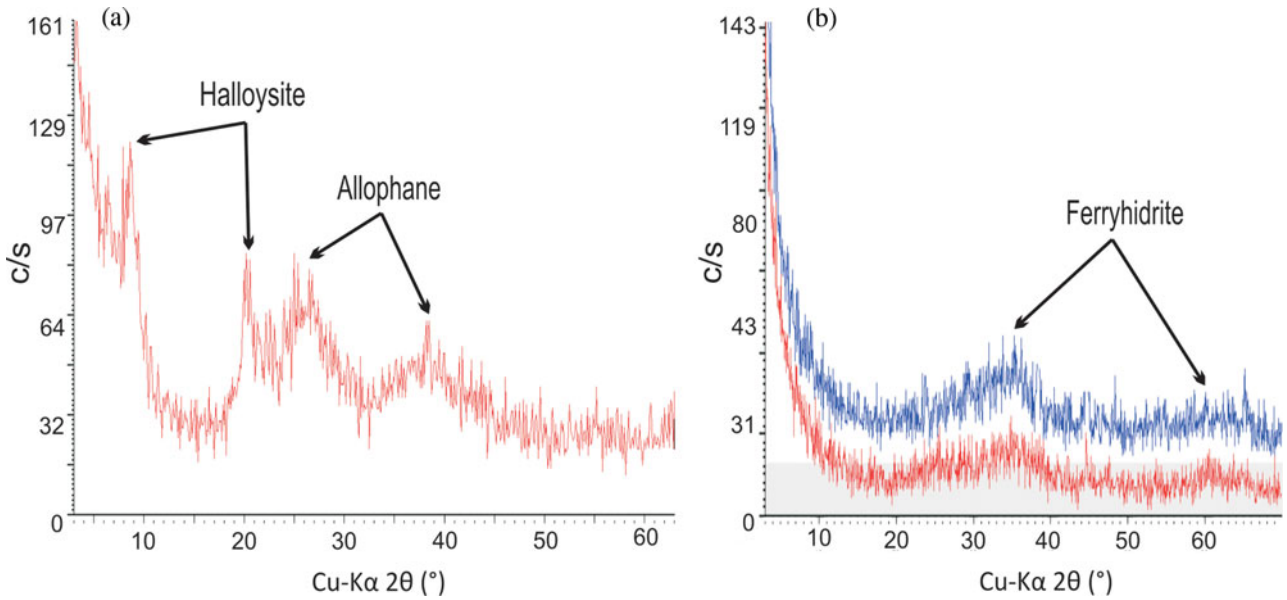

Figure 5. (Colour online) X-ray diffraction (XRD) patterns of: (a) a white hard rootsicle, showing allophane and halloysite peaks; and (b) a red hard rootsicle, showing the main Fe oxi-hydroxide band and small amounts of allophane (red line).

Those with a black exterior and yellow interior showed a diffuse and lumpy ringed structure (Fig. 4c). They contained relics of rotten roots.

5.a.4. Rootsicle distribution and cave water pH

The rootsicles showed a well-defined distribution in the lava tube (Fig. 2). The incipient and white hard rootsicles were found mostly in the left gallery within the first 40 m of the entrance of the lava tube, and also at specific points throughout the right gallery where the roof was closer to the ground surface (Fig. 2). The red hard rootsicles were found in the right gallery some 60 m from the entrance of the lava tube (Fig. 2), and were more abundant than the incipient and white hard rootsicles. The black spongy rootsicles appeared only in the right gallery in four places at 100, 150 and 250 m from the entrance and at the end of the gallery (Fig. 2).

The mean pH of the water in the cave (dripwater, runoff, small pools and puddles throughout the lava tube) was 6.83 ± 0.48. The dripwater associated with the incipient, white hard, red hard and black spongy rootsicles had a pH of 6.71, 6.57, 7.35 and 5.76, respectively.

5.b. Mineralogy

5.b.1. X-ray diffraction analysis

The degree of organization of the phases of the rootsicles was low and the XRD patterns very simple and weak, with broad bands that varied according to the studied zones. All the rootsicles were composed of poorly crystalline minerals that were more easily characterized in the hard rootsicles.

The XRD patterns of the white rootsicles showed two prominent bands: the first at 15–35° 2θ, peaking at 26–27° 2θ (3.3 Å), and another small band at 35–45° 2θ with a maximum at 40° 2θ (2.2 Å). Both correspond to allophane (Wada, 1989) (Fig. 5a). Allophane has no fixed chemical composition, and produces several XRD patterns (Childs, Matsue & Yoshinaga, 1990). The patterns studied by the latter authors revealed either Si-rich allophane (Al:Si = 1:1) or Al-rich allophane (Al:Si = 2:1), although the difference between these patterns was very small. In some of the present samples, the diffraction patterns showed two extra weak peaks at 8–9° 2θ (10.15 Å) and 20° 2θ (4.41 Å), probably due to the presence of small amounts of halloysite (Fig. 5a). Allophane was also identified in the incipient white hard and black spongy rootsicles.

XRD analysis of the red hard rootsicles revealed patterns with a scattering band peaking at 35–36° 2θ (2.50 Å), corresponding to poorly crystalline Fe oxi-hydroxides (Fig. 5b). In some cases, two incipient distinctive bands occurred: a main broad band, peaking at 35–36° 2θ (2.50 Å) and a small broad band peaking at 62–63° 2θ (1.49 Å) (Fig. 5b). Both bands define the presence of incipient '2-line' ferrihydrite (Jambor & Dutrizac, 1998). Both phases are referred to here as reflecting hydrous ferric oxi-hydroxide (HFO) minerals. These minerals were also identified in spots, patches and some rings in all rootsicles types.

5.b.2. Micro-Raman analysis

Micro-Raman spectrometry analysis of the rootsicles was performed to determine the characteristics of the carbonaceous matter (CM) and the composition of the black patches and layers not identified by XRD. The Raman spectra confirmed the presence of disordered CM, hausmannite and hisingerite (iron (III) phyllosilicate). The CM showed two vibrational bands in the exterior zone of the white hard rootsicles. The

https://doi.org/10.1017/S0016756814000491 Published online by Cambridge University Press

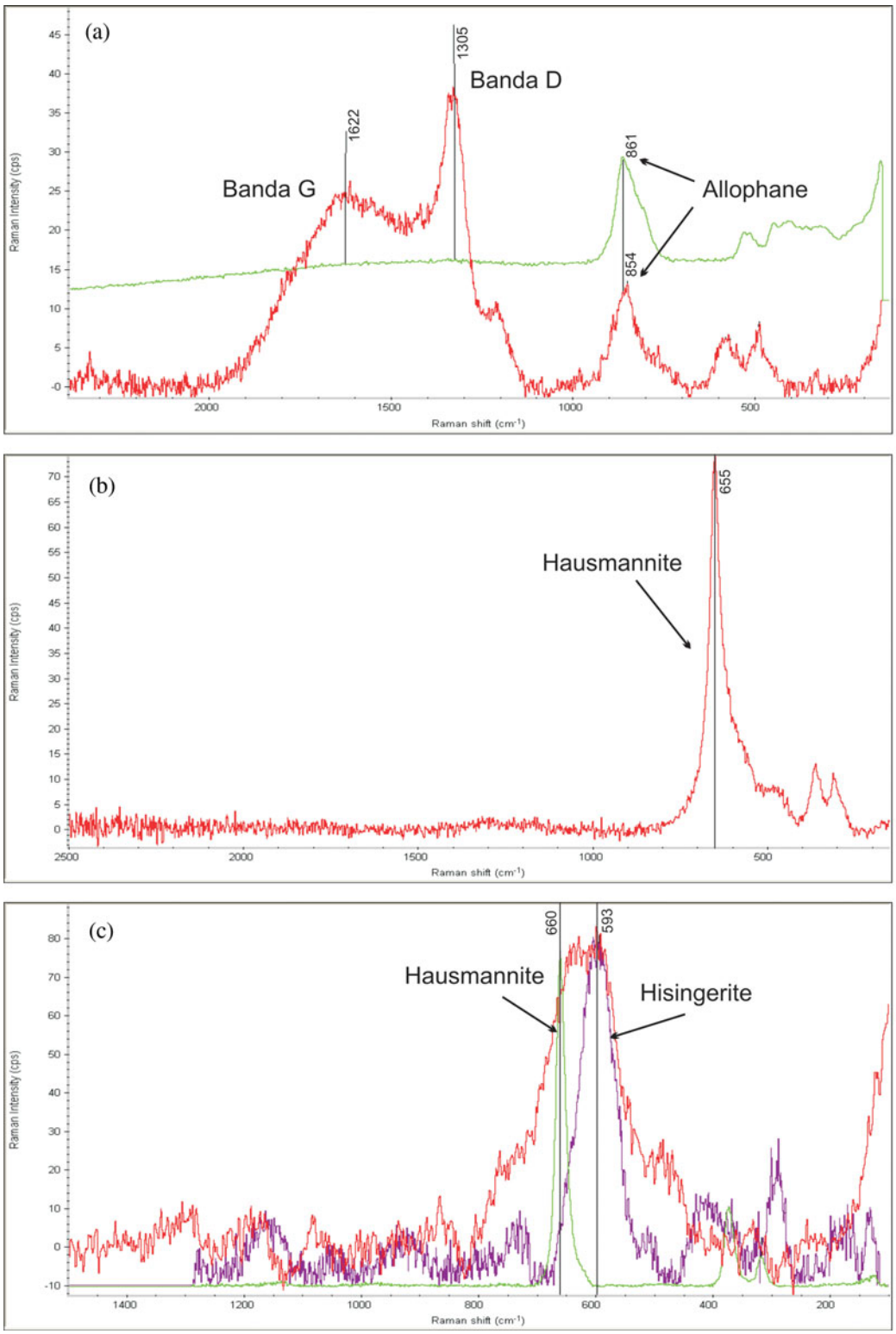

Figure 6. (Colour online) Raman spectra. (a) Spectrum for the external zone of a white hard rootsicle. The carbonaceous matter showed G and D vibrational bands that mix that for allophane (upper line). (b) Spectrum for a black layer showing the presence of hausmannite (peak at 665 cm^{-1}). (c) Spectrum of a black spot in which the hausmannite peak is the widest since it is mixed with that for hisingerite at around 590 cm^{-1}.

position of the prominent first band varied between 1300 and 1350 cm^{-1} (Fig. 6a) and corresponded to the commonly named D1 defect band (Beyssac *et al*. 2003). The wider, second band at around 1620 cm^{-1} (Fig. 6a) can be interpreted as the G band of the disordered CM, but with interference from a D2 band. In the brown and yellow interior part of the white hard rootsicles, the D1 band was the most important feature of the disordered CM. In some cases it was the only band (no D2/G was present). The CM bands were frequently accompanied by a peak at around 850 cm^{-1} corresponding to allophane (Fig. 6a).

https://doi.org/10.1017/S0016756814000491 Published online by Cambridge University Press

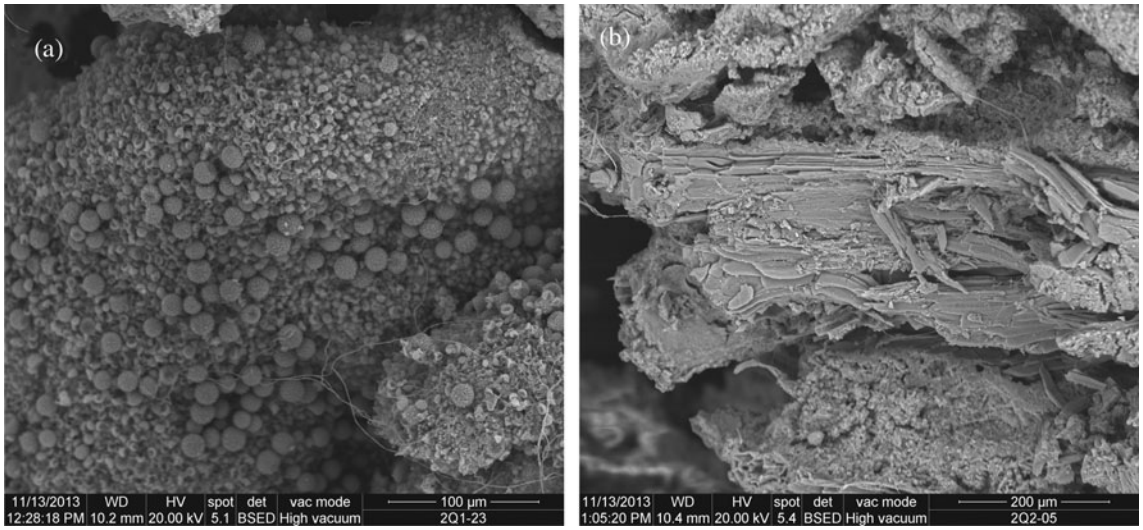

Figure 7. SEM images of incipient rootsicles: (a) exterior organic coat reveals a microbial component, mainly bacteria and fungi; and (b) well-preserved root tissues replaced by Si-rich allophane.

The Raman spectra of the black patches showed a peak at 650–660 cm^{-1} (Fig. 6b), sometimes along with those of the disorganized CM and allophane. This agrees with the Raman signal for hausmannite (Mn_3O_4), which consists of a very sharp peak at about 660 cm^{-1} (Julien *et al*. 2004; Mironova-Ulmane *et al*. 2009). In some spectra the hausmannite peak (660 cm^{-1}) was the widest since it was mixed with the hisingerite peak (590 cm^{-1}) (Fig. 6c).

5.c. SEM observations

5.c.1. Incipient rootsicles

The incipient rootsicles were formed by mineralized or rotten roots with an organic coating. This coating included a large microbial component mainly composed of bacteria, spores and fungi in the form of filaments, microspheres, pompons and biofilms (Fig. 7a). According to the EDX data, this organic component was mixed with the allophane.

The rootsicles sometimes showed well-preserved root tissues, totally or partially replaced by Si-rich allophane (Fig. 7b), as deduced from their EDX composition (atomic Al/Si ratio: 1.02 ± 0.08, atomic C/Si ratio: 2.54 ± 1.13). The rotten roots had a lumpy appearance; no root tissues were preserved. The lumpy masses of allophane microspheres (≤ 0.5 µm in diameter) were mixed with root relics. EDX analyses showed allophane rich in Si (atomic Al/Si ratio: 1.15 ± 0.15) plus minor elements such as Ca, Fe and Mn, and sporadically Na, Cl and Mg. Manganese oxides were present as scattered spheres/masses (5–15 µm in diameter).

5.c.2. Hard rootsicles

The three zones described in the white hard rootsicles (Fig. 4a) were studied by SEM. The exterior zone was composed of intercalations of compact thin rings (3–15 µm) with botryoidal surfaces, and porous rings formed mainly by partially or totally mineralized filaments (Fig. 8a). The compact rings were formed by allophane microspheres (≤ 0.5 µm in diameter), together producing botryoidal aggregates (Fig. 8a). EDX analyses showed the allophane to be rich in Al (atomic Al/Si ratio 1.86 ± 0.13) and often to include other minor elements such as Ca, Fe and Mn and sporadically Na, K, S and Cl. Cemented and thick mineralized filaments were observed at the base of these compact rings (Fig. 8b). The porous rings were composed of networks of partially (Fig. 8c) or totally (Fig. 8d) mineralized filaments and allophane microspheres. These microspheres fill any porosity, and cover and thicken the filaments (Fig. 8c). The black spots on the surface of some allophanic hard rootsicles were formed by lumpy reticular layers of manganese oxide and allophane spheres.

The intermediate zone was composed of thin allophanic rings mixed with many reticular manganese oxide spheres (Fig. 8e). These spheres were sometimes covered by biofilms and exopolysaccharides (EPS) (Fig. 8f), and found individually or in aggregates. EDX analyses showed these manganese oxide spheres to include minor elements such as Al, Si, Mn, Fe, Zn and Ce (Fig. 9a). Thin layers of manganese oxides were also seen between the thin allophanic rings (Fig. 9b).

The interior zone was formed of a mixture of root relics (Fig. 9c), allophane microspheres, reticular manganese oxide spheres, mineralized filaments, fungi, biofilms and EPS. The roots were either mineralized or rotten. Mineralized roots showed well-preserved tissues due to their partial or total replacement by allophane (Fig. 9d). The rotten roots were covered by many filaments, biofilms and EPS, all mixed with allophane microspheres and manganese oxide spheres (5–10 µm) (Fig. 9e). Sporadically, the filaments showed helical, stalked morphologies (*Gallionella s.p.*) and appeared within the vessels of the root tissues (Fig. 9f). Thin

https://doi.org/10.1017/S0016756814000491 Published online by Cambridge University Press

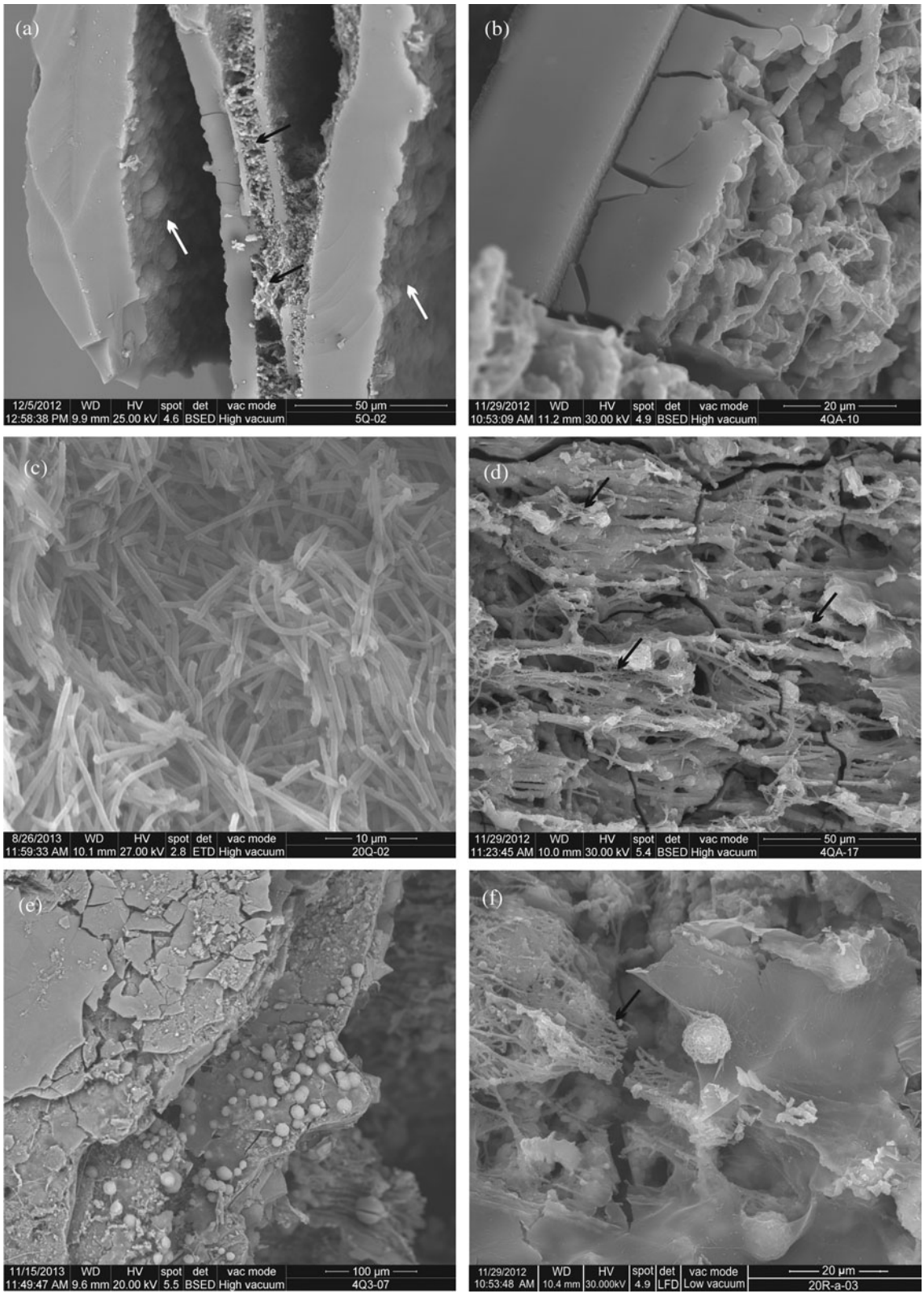

Figure 8. SEM images of white hard rootsicles. (a) Intercalation of compact and porous rings in the exterior zone. The botryoidal compact rings are formed from allophane microspheres that give rise to botryoidal aggregates (white arrows), plus porous rings formed by bacterial filaments mineralized by allophane (black arrows). (b) Detail of a bacterial filament ring at the base of a compact ring. The filaments are thicker and cemented with allophane, thus building up a more compact ring. (c) Networks of bacterial filaments in the porous rings, with a few replaced by allophane. (d) Networks of bacterial filaments totally replaced by allophane and showing exopolysaccharides (EPS) between them (black arrows). (e) Rings of the intermediate zone. Some allophanic rings showed many scattered spheres of manganese oxides. (f) Detail of the reticular manganese oxide spheres covered by biofilms and EPS (black arrow).

https://doi.org/10.1017/S0016756814000491 Published online by Cambridge University Press

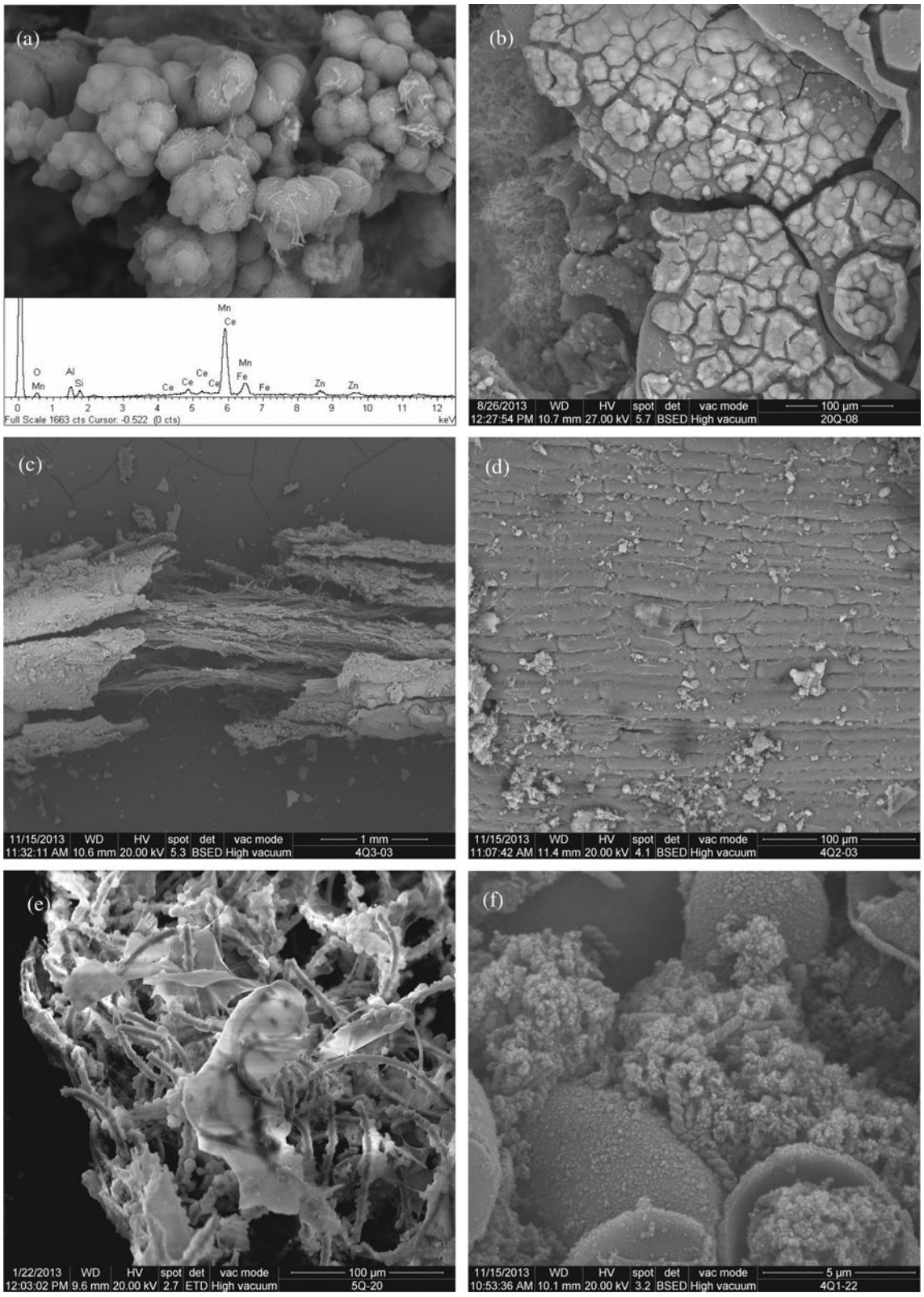

Figure 9. SEM images of white hard rootsicles. (a) Intermediate zone: layers of manganese oxides intercalated between the allophanic rings. (b) Close-up of (a). EDX spectra showed Al, Si, Mn, Fe, Zn and Ce to be incorporated into the spheres of manganese oxides. (c) The interior zone with root relics. (d) Mineralized root with well-preserved tissues. (e) Bacterial filaments, biofilms and EPS, mixed with allophane, covering a rotted root. (f) Bacterial filaments with helical morphologies (*Gallionella s.p.*) appear within the root vessels.

https://doi.org/10.1017/S0016756814000491 Published online by Cambridge University Press

layers of the manganese oxides sometimes surrounded the root remains. The microbial components and the rotten organic matter provided a wealth of C that showed up in the EDS analyses.

The red (ferric) hard rootsicles formed a structure of rings composed of intercalations of compact thin rings (4–10 μm) with botryoidal surfaces, and porous rings formed mainly from mineralized filaments (Fig. 10a).

The ferric minerals showed coalescence microspheres that formed botryoidal morphologies (Fig. 10b). EDX analyses revealed the ferric minerals to be rich in Si (atomic Fe/Si ratio: 4.11 ± 1.5) and to sometimes include other minor elements such as Ca, Co and Mn. The filaments showed mainly straight morphologies (*Lepthotrix* spp.; Fig. 10c) but also some helical forms (*Gallionella* spp.). Occasionally, small accumulations of allophane microspheres appeared between the bacterial filaments (Fig. 10c). Biofilms covered the ferric microspheres inside the porous rings (Fig. 10d). Layers with large accumulations of manganese oxides (Fig. 10e) were between the ring structures. Filaments encrusted by ferric minerals also occurred on Mn oxides (Fig. 10f). No relic root tissues were seen.

5.c.3. Black spongy rootsicles

The black spongy rootsicles showed masses and mineralized filaments of allophane with many reticular spheres and thin layers of Mn oxides (Fig. 11a). EDX analyses showed the allophane to be rich in Si (atomic Al/Si ratio: 1.03 ± 0.1). Other elements such as Fe, Ca and Mn, and sporadically Na, Ti, Mg and Cl, were sometimes included. The roots were partially rotten and showed well-preserved small vessels (Fig. 11b). The best-preserved root tissues were those partially or totally replaced by Si-rich allophane (atomic Al/Si ratio: 1.21 ± 0.08, C/Si: 3.50 ± 1.40).

6. Discussion

Field observations made at the Galeria da Queimada lava tube revealed the cave roof to be very near the surface of the ground (<0.5 m) and to be covered with volcanic soil. The soils of Terceira, mainly andisols, developed from young volcanic materials under damp temperate conditions (Pinheiro *et al*. 2004). Andisols have a colloid fraction dominated by amorphous and short-range-order materials such as allophane, imogolite, ferrihydrite and Al/Fe–humus complexes (Dahlgren, Saigusa & Ugolini, 2004). These minerals usually form during the early weathering of volcanic materials and some became constituents of the present rootsicles. These rootsicles were formed from infiltrating water that had passed through the soil covering the cave roof. This water would have become loaded with ions from the soil.

6.a. Mineralogical composition: organic versus inorganic precipitation

The incipient rootsicles, white hard rootsicles and black spongy rootsicles were found to be formed mainly of allophane (sometimes with minor halloysite), although the black spongy rootsicles also contained large amounts of Mn oxides. In contrast, the red hard rootsicles were composed mainly of HFO minerals. Mn oxides, and sometimes hisingerite, appeared as minor minerals in all the studied rootsicle types, forming black patches and thin layers or rings. Allophane and HFO minerals have several characteristics in common: (1) they are typical minerals of andisols; (2) they both have poorly ordered phases; (3) their morphologies under the SEM are similar (they have a fabric of microspheres that coalesce and form botryoidal aggregates), and (4) they form compact rings or rings associated with filaments, the shape and size of which are consistent with a bacterial origin (Jones, Renaut & Konhauser, 2005). The microspheres, which had a common structure, probably formed after shrinkage via the partial ordering of a gel that led to the expansion of voids (bubbles) and the partial ordering of the Fe/Si/Al-oxygen network (Eggleton, 1987). Much of the water contained in these non-crystalline minerals is probably found within these bubbles.

6.a.1. Allophane and halloysite formation

The allophane formation conditions in the rootsicles can be established from the data obtained for mineral soils. Dahlgren, Saigusa & Ugolini (2004) indicate that a pH of 5–7 promotes the formation of Al-polymers over Al–humus complexes, and that these Al-polymers react with silica to form allophane. The pH of the dripwater associated with the allophanic white and black rootsicles (6.57 and 5.76, respectively) falls within this interval. Wells *et al*. (1977) described the inorganic deposition of allophane in the stream channels of springs to be caused by a rise in pH on the loss of excess CO_2.

Few studies have emphasized the role of bacteria in the formation of allophane. Urrutia & Beveridge (1995) and Kawano & Tomita (2002) indicate that poorly ordered Al-Si or Al-Si-Fe minerals are produced on bacterial surfaces as a consequence of interaction with dissolved cations such as Al, Si and Fe. The organic polymers of the bacterial cell act as chemical absorbers as well as a template for the precipitation and growth of poorly ordered Al-Si-Fe minerals. According to the latter authors, in neutral conditions the silicate minerals developing on bacterial surfaces were probably formed by the binding of Si anions via bridging with metal ions bound to the cell surface via its net negative charge.

Halloysite was scarce in the studied rootsicles. Its localization in filamentous bacterial morphologies could not be distinguished by SEM given the small size of the mineral and because its own morphology is sometimes similar to that of bacterial filaments. Halloysite formation via bacterial mediation has been little

https://doi.org/10.1017/S0016756814000491 Published online by Cambridge University Press

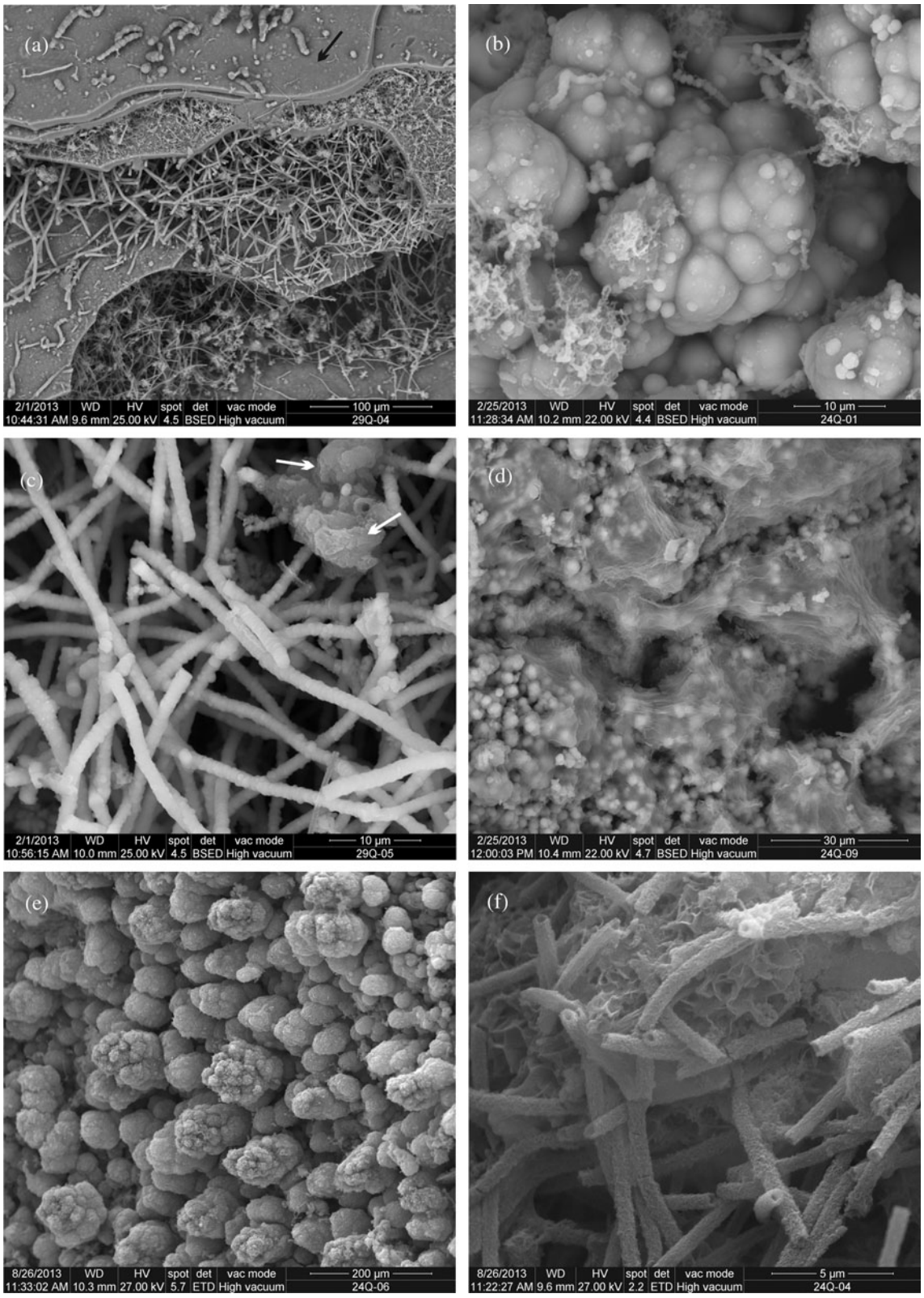

Figure 10. SEM images of red hard rootsicles. (a) Exterior zone with a ferric ring structure. This zone shows the intercalation of compact thin rings with botryoidal surfaces (black arrow) and porous rings formed by mineralized bacterial filaments. (b) Detail of botryoidal morphologies formed by ferric microspheres. (c) Small accumulations of allophane microspheres (white arrow) between the ferric bacterial filaments in the porous rings. (d) Biofilms covering ferric microspheres inside the porous rings. (e) Large accumulations of manganese oxides with botryoidal morphologies in the black spots of a red hard rootsicle. (f) Bacterial filaments encrusted by ferric minerals on reticulated accumulations of manganese oxides.

https://doi.org/10.1017/S0016756814000491 Published online by Cambridge University Press

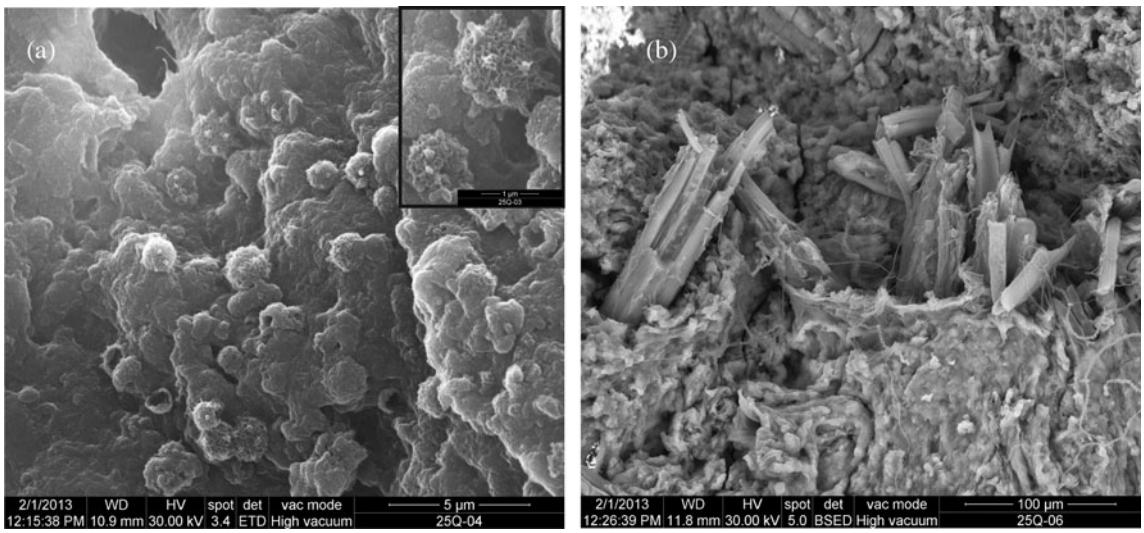

Figure 11. SEM pictures of two black spongy rootsicles. (a) Scattered spheres of manganese oxides in an allophanic mass. Close-up (right) showing the manganese oxide spheres. (b) Fragments of well-preserved allophanic root tissues inside the allophanic mass.

discussed in the literature, but the mechanism behind it may be similar to that of allophane formation. The term bio-halloysite was coined by Tazaki (2005) in studies of laboratory incubations of native minerals and resident microorganisms. This author reports a halloysite-like mineral to form on the cell walls of (tentatively) sulphate-reducing bacteria. Minyard *et al*. (2011) noted the presence of short nanotubes on cell surfaces in a saprolite sample, but fewer on the surrounding minerals. They suggested that cell surfaces may be the preferred sites for halloysite nucleation.

The bacterial genesis of halloysite cannot be clearly established for the present rootsicles since potential inorganic mechanisms exist: (1) the maturation of allophane (Bosák *et al*. 2002) and (2) its formation in preference to allophane when Si exceeds 10 mg L^{-1} or when annual rainfall is <1600 mm (Parfitt, 2009).

6.a.2. Ferric minerals (HFO minerals and hisingerite)

Ferrihydrite and other hydrated and hydroxylated iron oxide minerals occur widely in caves (Hill & Forti, 1997). Ferric rootsicles, formed mainly by Si-rich HFO minerals (incipient ferrihydrite and less-ordered hydrated oxi-hydroxides), are very extended throughout the Galeria Queimada lava tube. Ferrihydrite is often the predominant iron oxi-hydroxide formed in soils during the early weathering of all volcanic materials (Childs, Matsue & Yoshinaga, 1990) and its presence is significant in the soils of Terceira (Gérard *et al*. 2007). In the laboratory, 2-line ferrihydrite is prepared by the rapid oxidation of Fe (II) solutions or by the rapid neutralization of Fe (III) solutions. This occurs at ambient temperatures and at a pH of about 7 (Jambor & Dutrizac, 1998).

Phoenix *et al*. (2003) showed that bacterial cells immobilize more Fe than bacteria-free systems in solutions with iron concentrations of ≤50 ppm. However, as the concentration increases, non-bacterially-mediated precipitation begins to dominate. James & Ferris (2004) observed ochre-coloured bacteriogenic iron oxide precipitates to behave as potent substrates for ferric iron precipitation in a creek, with up to 75 % of total iron precipitated. Only 30 % of the total iron precipitated was under purely chemical control. These authors suggested that the macromolecular composition of the cell surfaces evolved as an ecophysiological strategy for obtaining maximum energy yields from Fe^{2+} oxidation via enhanced Fe^{3+} precipitation.

Hisingerite is an amorphous to poorly crystalline hydrated iron silicate that has been proposed as an early product of weathering in iron-rich volcanic deposits (Dahlgren, Saigusa & Ugolini, 2004). This mineral, detected by detailed micro-Raman analysis, occurred only in the black spots of incipient rootsicles and always associated with hausmannite. It was however scarce and probably formed by microbial activity. Iron silicates in conjunction with iron oxides have been found on bacterial surfaces (Fortin, Ferris & Scott, 1998). According to the latter authors, iron silicate formation involves a complex binding mechanism in which Fe forms bridges between the reactive sites on cell walls and silicate anions, thus initiating silicate nucleation.

6.a.3 Manganese oxides

Mn oxides produced by microbial activity are believed to be the most abundant and highly reactive Mn oxide phases in the environment. Microorganisms, especially bacteria but also fungi, are known to catalyse the oxidation of Mn (II) to form Mn (III, IV) oxide minerals (Tebo *et al*. 2004; Rossi *et al*. 2010). Several investigations have addressed the mechanisms of biological Mn (II) oxidation and biomineralization, with special interest shown in the possible existence of a Mn (III) intermediate (hausmannite) (Tebo *et al*. 2004). According to the latter authors, it is reasonable to think that bacteria first oxidize Mn (II) to Mn (III), and then Mn

https://doi.org/10.1017/S0016756814000491 Published online by Cambridge University Press

(III) is oxidized to Mn (IV). Hausmannite (Mn_3O_4) may be a primary product of the enzyme-catalysed Mn (II) oxidation reaction, which later transforms to Mn (IV) oxides abiotically.

6.b. Rootsicle genesis

The roots become a preferential site for the flow of seep water and, when environmental conditions (diffusion of CO_2 but also evaporation) are suitable, for guiding mineral deposition (Forti, 2001). This led to the formation of speleothems over roots (rootsicles), often showing anastomosis (Hill & Forti, 1997). Forti (2001) suggests that the interaction between a root and a growing speleothem might affect the morphology (passive effect) and chemical composition (active effect) of the latter.

6.b.1. Incipient rootsicles

In SEM/EDX analyses, the incipient rootsicles showed a mixture of organic matter and root tissues partially or totally replaced by allophane. Root putrefaction was observed. The organic and gelatinous cover on these rootsicles may be the microbial by-products of decomposition.

The literature contains little information on the replacement of roots by allophane in caves. However, this has been reported in some soils under humid and perhumid conditions and when the weathering environment is neutral to mildly acidic (Dahlgren, Saigusa & Ugolini, 2004). These conditions are similar to those found in the lava tube: the humidity is high and the pH of the dripwater varies from 5.76 to 7.35.

Martin & Lowe (1989) reported root residues with cell root structures preserved by allophane impregnation in a podzol; the present mineral replacement was similar, and tissue structures were preserved. Grathoff, Peterson & Beckstrand (2003) indicate that the residence time of water in woody material is very long, and that wood may serve as a semipermeable membrane that facilitates initial replacement by allophane. The microbial by-products of root decomposition could help in such replacements (Buurman, Peterse & Almendros Martin, 2007; Parfitt, 2009). Kawano & Tomita (2002) report that allophane minerals may precipitate rapidly as an early stage product due to the presence of bacteria.

The incipient rootsicles grow via the laying down of rings of poorly crystalline minerals, forming hard rootsicles.

6.b.2. Hard rootsicles

The hard rootsicles have a central zone of partially or totally mineralized root material and an outer zone composed of concentric rings of allophane or HFO minerals, frequently rich in Si (according to the EDX data).

SEM observations of the white and red hard rootsicles showed that thin compact rings, formed by inorganic precipitation, are interspersed by rings comprising bacterial filaments with different morphologies. Sometimes bacterial filament rings, initially porous, became progressively cemented and end up as compact rings. Micro-Raman analysis revealed well-developed D1 and D2/G bands of organic matter, a consequence of the presence of large microbial communities inside the ring structures.

In the white hard rootsicles, inorganic allophane precipitation occurred when the meteoric water (acidified by the presence of soil-derived CO_2) infiltrated the present lava tube. The acidic solutions, rich in Si and Al, reached the ceiling of the cave and a rapid neutralization occurred via the degassing of CO_2, resulting in the inorganic precipitation of allophane. Plant roots may also play an active role in allophane precipitation, notably by causing localized see-saw changes in the CO_2 levels in those areas adjacent to them. The same is seen in calcite precipitation in carbonate rootsicles (Forti, 2001; Taboroši, Hirakawa & Stafford, 2004). The intermediate zone in the white hard rootsicles can be interpreted as reflecting the relationship between the root and the surrounding precipitation environments, as seen in soil rizhocretions.

In the white hard rootsicles, the allophanic porous rings are formed by undetermined bacterial filaments. In the red hard rootsicles, the morphology of the filaments is similar to that of others (attributed to *Leptothrix* spp. and *Gallionella* spp.) in the speleothems of the nearby Buracos lava tube (De los Ríos *et al*. 2011). Both types of bacteria can extract metabolic energy via Fe (II) oxidation under neutral pH conditions. Bacterial activity seems to be clearly involved in red hard rootsicle formation, although inorganic HFO mineral precipitation also occurs to form compact rings. The pH of the dripwater associated with the red hard rootsicles was around 7.35, which would favour both the inorganic (Jambor & Dutrizac, 1998) and organic precipitation of HFO minerals. During periods when the Fe concentration of the dripwater reaches >50 ppm, inorganic HFO mineral precipitation would be favoured over bacterial precipitation (Phoenix *et al*. 2003).

Red hard (HFO minerals) and white (allophane) hard rootsicles clearly develop in different parts of the cave. Indeed, nearly all of the white types are found in the left gallery and most of the red types in the right gallery (see Fig. 2). This might be explained by: (1) differences in the proximity of the lava tube roof to the surface (the incipient and white rootsicles are located in areas where the lava tube roof is closer to the surface than in the red rootsicle area); or (2) the characteristics of the surface located above the lava tube (plant cover, amount of water present, etc.). The surface conditions above a lava tube may directly influence the pH, organic matter and colloidal composition of an andisol (Dahlgren, Saigusa & Ugolini, 2004). The red rootsicles are mainly located below waterlogged areas with small, ephemeral surface ponds and, in many cases, beneath pasture. These same conditions have been observed on the surface above other lava tubes on the island (e.g.

https://doi.org/10.1017/S0016756814000491 Published online by Cambridge University Press

the Buracos or Balcões caves; F. Pereira, pers. comm., 2012) and their speleothems are also formed from Fe oxi-hydroxides (De los Ríos *et al.* 2011). The surface of the left gallery coincides mainly with the boundary of pasture fields, where there is a strong concentration of plants and shrubs (hydrangeas, brambles, ferns, etc.).

6.b.3. Black spongy rootsicles

These show a central zone with a partially or totally mineralized root, plus an outer zone made up of allophane and Mn oxides. Scattered spheres, masses and thin layers of Mn oxides, and sometimes hausmannite (according to the micro-Raman data), were found.

The Mn oxides incorporate minor elements such as Al, Si, Fe, Zn and Ce. Of these, the most interesting are Zn and Ce since their incorporation may indicate a biogenic origin. Miyata *et al*. (2007) indicate that biogenic Mn oxides produced by bacteria have structurally less Mn (III), compensated for by exchangeable charge-balancing cations. Mn-oxidizing bacteria have a suit of enzymes that not only help to scavenge Mn but also associated elements such as Zn (Toner *et al*. 2006). Ce was preferentially incorporated over other rare Earth elements (REEs) into the Mn oxides studied; this might be attributed to the oxidative scavenging of dissolved Ce (III) by Mn oxides. Microorganisms would facilitate this incorporation via specific redox events (Tanaka *et al*. 2010).

The black spongy rootsicles, formed by allophane and Mn oxides but no HFO minerals, are largely located in a specific area of the lava tube (Fig. 2) corresponding to intersections of pasture fields at the surface. In this area there is thick tree cover (*Cryptomeria japonica*) (Dias, Elias & Nunes, 2004).

7. Conclusions

The root-associated stalactites (rootsicles) found in the Galeria da Queimada lava tube are not particularly common since they are formed mainly of allophane, HFO minerals and Mn oxide minerals (the vast majority of rootsicles seen around the world are composed of calcite). Their mineralogical composition and developmental association with microbes render them unique. These rootsicles provide an excellent opportunity for the study of biomineralization induced by microbial activity in caves, especially with respect to allophane; this has never before been described in caves.

The Galeria da Queimada lava tube is home to three rootsicle types – incipient, hard (white and red) and black spongy – of different mineralogy, texture and structure. Allophane, HFO minerals and Mn oxides, typical of andisols (the soil type covering the lava tube roof), precipitated from the dripwater running along the roots and formed all these rootsicles.

Incipient rootsicles are the first step in rootsicle formation. Those inspected showed the microbial products of root putrefaction and the initial replacement of plant tissues by allophane. The microbial by-products of plant decomposition could help in such replacement. The role of the roots themselves in rootsicle formation is unclear, although they can cause localized changes in dripwater CO_2 levels and thus enhance the initial inorganic precipitation of allophane via the resulting pH changes.

The hard rootsicles (the most developed) have a central zone with partially or totally mineralized roots plus an exterior zone made up of many concentric rings composed of allophane and/or Si-rich HFO minerals. In the white hard rootsicles, the intermediate zone was interpreted as a consequence of the relationship between the root and the surrounding precipitation environment, as seen in soil rizhocretions. The alternation of organic and inorganic precipitation of allophane and Si-rich HFO minerals builds up the ring structure. Organic precipitation is facilitated by bacteria (observed in large quantities in SEM images), which appear as filamentous structures. Some porous bacterial rings become progressively cemented and eventually compact. The changes in the pH of the dripwater and in the cave temperature would favour the inorganic precipitation of allophane and HFO minerals in compact rings, although most precipitation would be bacterially induced.

The mainly straight filament morphologies are indicative of *Leptothrix* spp. The helical morphologies seen (in much smaller numbers) in the ferric rootsicles might be indicative of *Gallionella* spp. In general, organic matter (roots and their decomposition products) and bacterial activity leave their mark in the rootsicles as G and D bands in the CM detected by micro-Raman analysis.

The black spongy rootsicles, formed mainly from allophane and Mn oxides, conserve rotten root material. It is reasonable to hypothesize that microorganisms (especially bacteria), but also fungi, catalyse the oxidation of Mn (II) to form Mn (III, IV) oxide minerals. Zn and Ce were incorporated into these manganese oxides, probably also as a consequence of microbial activity. Mn oxide minerals, and occasionally hisingerite, appear as black patches, spots and thin layers in all the types of rootsicle examined.

The white hard, red hard and black spongy rootsicles develop preferentially in different parts of the cave. The surface conditions above the cave roof (pasture fields, or boundaries between these and dense vegetation), may influence the type of rootsicle found. These soils may be of different pH, contain different amounts of organic matter or differ in their colloidal composition, for example. The red hard rootsicles are mainly located under areas of pasture with waterlogged soils and small ponds. The white hard and black spongy rootsicles are mainly located where the roof is close to the surface and where the surface vegetation (hydrangeas, brambles, ferns, etc.) is dense along the boundaries of pasture fields.

Acknowledgements. This work was funded by Project CGL2011-27826-CO2-02 from the Spanish Ministry of Science and Innovation. R.D. was supported by a CSIC

JAE-Predoc grant co-financed by the European Social Fund (ESF).The authors are grateful to Fernando Pereira of the *Associação Os Montanheiros*, Terceira for local logistic support to C. Riquelme of the University of Terceira and fieldtrip support to F. Sánchez. L. Tormo, M. Furió and A.J. García of the Non-Destructive Analytical Techniques Laboratory at the *Museo Nacional de Ciencias Naturales* (CSIC), Madrid are thanked for assistance with SEM-EDS-WDS. We thank an anonymous reviewer and Dr Paolo Forti for their detailed review of the manuscript. We thank A. Burton for editing and language assistance.

References

BARTON, H. A. & NORTHUP, D. E. 2007. Geomicrobiology in cave environments: past, current and future perspectives. *Journal of Cave & Karst Studies* **69**, 163–78.

BEYSSAC, O., GOFFÉ, B., PETITET, J.-P., FROIGNEUX, E., MOREAU, M. & ROUZAUD, J.-N. 2003. On the characterization of disordered and heterogeneous carbonaceous materials by Raman spectroscopy. *Spectrochimica Acta Part A: Molecular & Biomolecular Spectroscopy* **59**, 2267–76.

BORGES, P. A. V., PEREIRA, F. & SILBER, A. 1992. Grutas e algares dos Açores. I. Seis novas topografías de tubos de lava fa ilha Terceira. In *Espeleológica, O.M.S.d.E. 3º Congresso Nacional de Espeleologia e do 1º encontro Internacional de Vulcanoespeleologia das Ilhas Atlanticas: Lisboa-Portugal*, pp. 2–26.

BORGES, P. A., SILVA, A. & PEREIRA, F. 1992. Caves and pits from the Azores with some comments on their geological origin, distribution and fauna. In *Proceedings of the 6th International Symposium on* Vulcanospeleology, Hilo, Hawaii. National Speleological Society, pp. 121–51.

BOSÁK, P., BELLA, P., CILEK, V., FORD, D. C., HERCMAN, H., KADLEC, J., OSBORNE, A. & PRUNER, P. 2002. Ochtiná Aragonite Cave (Slovakia): morphology, mineralogy and genesis. *Geologica Carpathica* **53**, 399–410.

BOSTON, P. J., SPILDE, M. N., NORTHUP, D. E., MELIM, L. A., SOROKA, D. S., KLEINA, L. G., LAVOIE, K. H., HOSE, L. D., MALLORY, L. M., DAHM, C. N., CROSSEY, L. J. & SCHELBLE, R. T. 2001. Cave biosignature suites: microbes, minerals, and Mars. *Astrobiology* **1**, 25–55.

BUURMAN, P., PETERSE, F. & ALMENDROS MARTIN, G. 2007. Soil organic matter chemistry in allophanic soils: a pyrolysis-GC/MS study of a Costa Rican &osol catena. *European Journal of Soil Science* **58**, 1330–47.

CALVERT, A. T., MOORE, R. B., MCGEEHIN, J. P. & RODRIGUES DA SILVA, A. M. 2006. Volcanic history and 40Ar/39Ar and 14C geochronology of Terceira Island, Azores, Portugal. *Journal of Volcanology and Geothermal Research* **156**, 103–15.

CASTAÑO, R., REDONDO VEGA, J. & FERNÁNDEZ MARTÍNEZ, E. 2010. La cueva de Valdelajo (Sahelices de Sabero, León): una pequeña joya geológica en una comarca minera. In *Una Visión Multidisciplinar del Patrimonio Geológico y Minero* (eds P. F. e. I. Rábano), pp. 47–61. Cuadernos del Museo Geominero. Madrid, Instituto Geológico y Minero de España.

CHILDS, C. W., MATSUE, N. & YOSHINAGA, N. 1990. Ferrihydrite in volcanic ash soils of Japan. *Soil Science and Plant Nutrition* **37**, 299–311.

DAHLGREN, R. A., SAIGUSA, M. & UGOLINI, F. C. 2004. The nature, properties and management of volcanic soils. *Advances in Agronomy* **82**, 113–82.

DAZA, R. & BUSTILLO, M. A. 2013. Mineralogía de los bioespeleotemas de la "Galeria da Queimada" (Terceira, Azores). *Macla* **17**, 43–4.

DE LOS RÍOS, A., BUSTILLO, M. A., ASCASO, C. & CARVALHO, M. R. 2011. Bioconstructions in ochreous speleothems from lava tubes on Terceira Island (Azores). *Sedimentary Geology* **236**, 117–28.

DIAS, E., ELIAS, R. B. & NUNES, V. 2004. Vegetation mapping and nature conservation: a case study in Terceira Island (Azores). *Biodiversity and Conservation* **13**, 1519–39.

EGGLETON, R. A. 1987. Noncrystalline Fe-Si-Al-oxyhydroxides. *Clays and Clay Minerals* **35**, 29–37.

FORTI, P. 2001. Biogenic speleothems: an overview. *International Journal of Speleology* **30**, 39–56.

FORTI, P. 2005. Genetic processes of cave minerals in volcanic environments: an overview. *Journal of Cave and Karst Studies* **67**, 3–13.

FORTIN, D., FERRIS, F. G. & SCOTT, S. D. 1998. Formation of Fe-silicates and Fe-oxides on bacterial surfaces in samples collected near hydrothermal vents on the Southern Explorer Ridge in the northeast Pacific Ocean. *American Mineralogist* **83**, 1399–408.

FRANÇA, Z., CRUZ, J. V., NUNES, J. C. & FORJAZ, V. H. 2003. Geologia dos Açores: uma perspectiva actual. *Açoreana* **10**, 11–140.

GÉRARD, M., CAQUINEAU, S., PINHEIRO, J. & STOOPS, G. 2007. Weathering and allophane neoformation in soils developed on volcanic ash in the Azores. *European Journal of Soil Science* **58**, 496–515.

GRATHOFF, G., PETERSON, C. & BECKSTRAND, D. 2003. Coastal dune soils in Oregon, USA, forming allophane, imogolite and gibbsite. In *2001. A Clay Odyssey*, pp. 197–204. Proceedings of the 12th International Clay Conference, Bahia Blanca.

HILL, C. A. 1999. Mineralogy of Kartchner Caverns, Arizona. *Journal of Caves and Karst Studies* **61**, 73–8.

HILL, C. A. & FORTI, P. 1997. *Cave Minerals of the World*. Alabama, USA, National Speleological Society, Huntsville, 463 pp.

JAMBOR, J. L. & DUTRIZAC, J. E. 1998. Occurrence and constitution of natural and synthetic ferrihydrite, a widespread iron oxyhydroxide. *Chemical Reviews* **98**, 2549–86.

JAMES, R. E. & FERRIS, F. G. 2004. Evidence for microbial-mediated iron oxidation at a neutrophilic groundwater spring. *Chemical Geology* **212**, 301–11.

JAMES, J., JENNINGS, J. & DYSON, H. 1982. Mineral decoration and weathering of the caves: Wombeyan Caves. *Sydney Speleological Society* **8**, 121–36.

JASINSKA, E. J., KNOTT, B. & MCCOMB, A. J. 1996. Root mats in ground water: a fauna-rich cave habitat. *Journal of the North American Benthological Society* **15**, 508–19.

JONES, B., RENAUT, R. & KONHAUSER, K. 2005. Genesis of large siliceous stromatolites at Frying Pan Lake, Waimangu geothermal field, North Island, New Zealand. *Sedimentology* **52**, 1229–52.

JULIEN, C. M., MASSOT, M. & POINSIGNON, C. 2004. Lattice vibrations of manganese oxides: Part I. Periodic structures. *Spectrochimica Acta Part A: Molecular and Biomolecular Spectroscopy* **60**, 689–700.

KASAMA, T. & MURAKAMI, T. 2001. The effect of microorganisms on Fe precipitation rates at neutral pH. *Chemical Geology* **180**, 117–28.

KAWANO, M. & TOMITA, K. 2002. Microbiotic formation of silicate minerals in the weathering enviroment of a pyroclastic deposit. *Clays and Clay Minerals* **50**, 99–110.

MARTIN, D. E. & LOWE, L. E. 1989. Characterization and classification of root mat horizons in some coastal British Columbia podzols. *Canadian Journal of Soil Science* **69**, 17–23.

MINYARD, M. L., BRUNS, M. A., MARTÍNEZ, C. E., LIERMANN, L. J., BUSS, H. L. & BRANTLEY, S. L. 2011. Halloysite nanotubes and bacteria at the saprolite–bedrock interface, Rio Icacos Watershed, Puerto Rico. *Soil Science of Society America Journal* **75**, 348–56.

MIRONOVA-ULMANE, N., KUZMIN, A. & GRUBE, M. 2009. Raman and infrared spectromicroscopy of manganese oxides. *Journal of Alloys and Compounds* **480**, 97–9.

MIYATA, N., TANI, Y., SAKATA, M. & IWAHORI, K. 2007. Microbial manganese oxide formation & interaction with toxic metal ions. *Journal of Bioscience and Bioengineering* **104**, 1–8.

NORTHUP, D. E., MELIM, L. A., SPILDE, M. N., HATHAWAY, J. J. M., GARCIA, M. G., MOYA, M., STONE, F. D., BOSTON, P. J., DAPKEVICIUS, M. L. N. E. & RIQUELME, C. 2011. Lava cave microbial communities within mats and secondary mineral deposits: implications for life detection on other planets. *Astrobiology* **11**, 601–18.

NUNES, J. C. 2000. Notas sobre a geologia da Ilha Terceira. *Açoreana* **9**, 205–15.

NUNES, J. C. 2004. Geologia, vulcanismo e sismologia. In *Atlas Básico dos Açores* (ed. V. H. Forjaz). Observatório Vulcanológico e Geotérmico dos Açores, Ponta Delgada.

NUNES, J. C., GARCIA, P., LIMA, E. A., COSTA, M. P. & PEREIRA, F. 2008. New geological insights for the Azores Islands (Portugal) Lava Caves. *XIII International Symposium on Vulcanospeleology*, 1–10 September, Korea.

PARFITT, R. L. 2009. Allophane and imogolite: role in soil biogeochemical processes. *Clay Minerals* **44**, 135–55.

PHOENIX, V. R., KONHAUSER, K. O. & FERRIS, F. G. 2003. Experimental study of iron and silica immobilization by bacteria in mixed Fe-Si systems: implications for microbial silicification in hot springs. *Canadian Journal of Earth Sciences* **40**, 1669–78.

PINHEIRO, J. 2012. Caracterização geral dos solos da ilha Terceira (Açores) que se enquadram na Ordem andisol. In V Congresso Ibérico da Ciência do Solo 2012. *Guia de Campo. Excursão técnico-científica. Os Andossolos da ilha Terceira e paisagens associadas*, pp. 26–41.

PINHEIRO, J., SALGUERO, M. T. & RODRIGUEZ, A. 2004. Genesis of placic horizons in andisols from Terceira Island Azores, Portugal. *Catena* **56**, 85–94.

ROSSI, C., LOZANO, R. P., ISANTA, N. & HELLSTROM, J. 2010. Manganese stromatolites in caves: El Soplao (Cantabria, Spain). *Geology* **38**, 1119–22.

SELF, S. & GUNN, B. 1976. Petrology, volume and age relations of alkaline and saturated peralkaline volcanics from Terceira, Azores. *Contributions to Mineralogy and Petrology* **54**, 293–313.

TABOROŠI, D., HIRAKAWA, K. & STAFFORD, K. 2004. Interactions of plant roots and speleothems. *Journal of Subterranean Biology* **2**, 43–51.

TAMAS, T. & UNGUREANU, R. 2010. Mineralogy of speleothems from four caves in the Purcăreţ-Boiu Mare Plateau and the Baia Mare Depression (NW Romania). *Studia Universitatis Babeş-Bolyai, Geologia* **55**, 43–9.

TANAKA, K., TANI, Y., TAKAHASHI, Y., TANIMIZU, M., SUZUKI, Y., KOZAI, N. & OHNUKI, T. 2010. A specific Ce oxidation process during sorption of rare earth elements on biogenic Mn oxide produced by Acremonium sp. strain KR21–2. *Geochimica et Cosmochimica Acta* **74**, 5463–77.

TAZAKI, K. 2005. Microbial formation of halloysite-like mineral. *Clays and Clay Minerals* **53**, 224–33.

TEBO, B. M., BARGAR, J. R., CLEMENT, B. G., DICK, G. J., MURRAY, K. J., PARKER, D., VERITY, R. & WEBB, S. M. 2004. Biogenic manganese oxides: properties and mechanisms of formation. *Annual Review Earth Planetary Science* **32**, 287–328.

TONER, B., MANCEAU, A., WEBB, S. M. & SPOSITO, G. 2006. Zinc sorption to biogenic hexagonal-birnessite particles within a hydrated bacterial biofilm. *Geochimica et Cosmochimica Acta* **70**, 27–43.

URRUTIA, M. M. & BEVERIDGE, T. J. 1995. Formation of short-range ordered aluminosilicates in the presence of a bacterial surface (Bacillus subtilis) and organic ligands. *Geoderma* **65**, 149–65.

WADA, K. 1989. Allophane and imogolite. In *Minerals in Soil Environments*, 2nd edition (eds J. B. Dixon and S. B. Weed), pp. 1051–1087. Soil Science Society of America, Madison, WI.

WELLS, N., CHILDS, C. W. & DOWNES, C. J. 1977. Silica Springs, Tongariro National Park, New Zealand-analyses of the spring water and characterisation of the alumino-silicate deposit. *Geochimica et Cosmochimica Acta* **41**, 1497–506.